International Journal of Heat and Mass Transfer 51 (2008) 4966–4972

Contents lists available at ScienceDirect

International Journal of Heat and Mass Transfer

journal homepage: www.elsevier.com/locate/ijhmt

A new methodology of studying the dynamics of water sorption/desorption under real operating conditions of adsorption heat pumps: Experiment

Yu.I. Aristov [a,*], B. Dawoud [b], I.S. Glaznev [a], A. Elyas [c]

[a] Boreskov Institute of Catalysis, Pr. Lavrentieva 5, Novosibirsk 630090, Russia
[b] Viessmann GmbH and Co. KG, D-35107 Allendorf/Eder, Germany
[c] Aachen University of Technology (RWTH-Aachen), Chair of Technical Thermodynamics, Schinkel Str. 8, D-52056 Aachen, Germany

ARTICLE INFO

Article history:
Received 22 December 2006
Received in revised form 25 September 2007
Available online 29 April 2008

Keywords:
Adsorption heat pumps
Sorption kinetics
Coupled heat and mass transfer
Selective water sorbent
Silica gel
Calcium chloride

ABSTRACT

In this paper we proposed and tested a new methodology of studying the kinetics of water vapour sorption/desorption under operating conditions typical for isobaric stages of sorption heat pumps. The measurements have been carried out on pellets of composite sorbent SWS-1L ($CaCl_2$ in silica KSK) placed on a metal plate. Temperature of the plate was changed as it takes place in real sorption heat pumps, while the vapour pressure over the sorbent was maintained almost constant (saturation pressures corresponding to the evaporator temperature of 5 °C and 10 °C and the condenser temperature of 30 °C and 35 °C). Near-exponential behaviour of water uptake on time was found for most of the experimental runs. Characteristic time τ of isobaric adsorption (desorption) was measured for one layer of loose grains having a size between 1.4 mm and 1.6 mm for different heating/cooling scenarios and boundary conditions of an adsorption heat pump. Maximum specific power estimated from the τ-values can exceed 1.0 kW/kg of dry adsorbent, that gives proof to the idea of compact adsorption units for energy transformation with loose SWS grains.

1. Introduction

Lang et al. [1] have proposed a design of the adsorber heat exchanger, in which a mono-layer of loose pellets of an adsorbent is placed on the surface of the fins of a finned tube heat exchanger. This design has proven itself to be effective during the investigations of a multi-modular adsorption heat pump (AHP), carried out by Stricker [2]. The dynamics of water sorption was studied for such configuration in a constant volume – variable pressure unit under three different initial conditions typical for the operation of adsorption heat pumps (60 mbar, 50 °C), (40 mbar, 50 °C) and (40 mbar, 35 °C) [3,4]. The first paper presented an experimental study on the kinetics of water vapour sorption on two host materials (mesoporous silica-gel KSK and alumina A1) in comparison with the two composites SWS-1L and SWS-1A formed by impregnating these two host matrices with $CaCl_2$. The initial states of water vapour in the vapour vessel (A) and of the sorbent sample in the measuring cell (B) of a typical sorption process realised in these experiments are presented on the Clausius-Clapeyron diagram together with the single-effect adsorption cycle plotted for SWS-1L (Fig. 1). At the beginning of the experiments the loose grains of the sample were almost completely dry (residual uptake $x_o = 0.0017$ g/g) and maintained at initial adsorption temperature 35 °C (or 50 °C), that corresponds to point (B) in Fig. 1. After that, the sample was subjected to a step change of the vapour pressure up to 40 mbar (or 60 mbar), which initiated the sorption process in the constant volume apparatus. The vapour pressure was decreasing due to water sorption. Depending on the size of the grains and the configuration of the sorbent layer (single or multi layer) the sorption process can be isothermal (solid line in Fig. 1) or non-isothermal. The final equilibrium state of the sorbent can be expected on the isothermal line between points A and B depending on the sample mass, starting pressure and the volume of the vapour vessel. Measuring the temporal evolution of pressure $p(t)$, the time variation of the water loading was calculated. The sorption of water lasted some tens of minutes until the equilibrium was reached. As the pressure jump was large (non-isothermal adsorption) and the pressure was not constant during the water adsorption, no simple kinetic models could be applied for extracting kinetic parameters from the experimental curves. However, this simple qualitative procedure could be used for comparative study of various sorbents under the prescribed boundary conditions. To make the comparison, the sorption rate was characterized by times $\tau_{\chi=0.5}$ and $\tau_{\chi=0.9}$ for reaching 50% and 90% of the equilibrium loading. The maximum half-time of water sorption $\tau_{\chi=0.5} = 4.85$ min. was measured for composite SWS-1A ($CaCl_2$ in alumina) at $p_o(H_2O) = 60$ mbar and $T = 50$ °C [3]. The fastest sorption ($\tau_{\chi=0.5} = 1.0$ min) was found for pure mesoporous silica at $p_o(H_2O) = 40$ mbar and $T = 50$ °C [3]. The kinetic curves were non-exponential

* Corresponding author. Tel./fax: +7 383 330 95 73.
E-mail address: aristov@catalysis.ru (Yu.I. Aristov).

0017-9310/$ - see front matter © 2008 Elsevier Ltd. All rights reserved.
doi:10.1016/j.ijheatmasstransfer.2007.10.042

Nomenclature

d	differential operator (minus)
E_{act}	activation energy (J/mol)
h_{fg}	latent heat of vaporization (kJ/kg)
k	rate constant (s^{-1})
m	mass (kg)
$\dot{m}$	mass flow rate (kg s^{-1})
N	water loading (mol_{H_2O}/mol_{CaCl_2})
p	pressure (kPa)
R	gas constant (kJ kg^{-1} K^{-1})
S	internal surface area of the porous sorbent (m^2)
t	time (s)
T	temperature (K)
V	volume (m^3)
x	water loading (g/g)
W	specific power (kW/kg or W/kg)

Greek symbols

Δ	difference operator (−)
Φ	pore diameter (nm)
ϑ	temperature (°C)
τ	characteristic time (s)
χ	dimensionless differential water loading (−)

Subscripts

1–4	state points in Fig. 1
0	initial value
ads	adsorbent
amb	ambient
con	condenser
des	desorber
ev	evaporator
f	final value
max	maximum
MC	measuring cell
s	sorbed
sor	sorber
S, dry	dry sample
t	instantaneous value
VV	vapor vessel
WV	water vapor

with a long tail at large times, so that typically $\tau_{\chi=0.9}$ was 5–8 times larger than $\tau_{\chi=0.5}$. This allowed the estimation of the average cooling power generated during the adsorption phase [4]. Similar test rig was reported in [5,6] with useful addition of a heat flux meter to measure the released heat of adsorption as well as the sample surface temperature during the adsorption process.

Although, sorbents with smaller $\tau_{\chi=0.5}$ and $\tau_{\chi=0.9}$ can be recommended for applying in AHPs with a short working cycle, so measured characteristic times can not be directly used for estimating the duration of the isobaric adsorption and desorption stages (4–1 and 2–3 in Fig. 1). Indeed, the adsorption process B-1 realized in Refs. [3,4] was induced by a jump of pressure at a quasi-constant temperature, while in an AHP it is initiated by the drop of sorbent temperature at a quasi-constant pressure maintained by an evaporator.

In this paper we proposed and tested a new quantitative methodology for studying the dynamics of water sorption under operating conditions close to those realized during isobaric stages of an AHP. Characteristic times of isobaric adsorption (desorption) were measured for a one layer of lose grains (size 1.4–6 mm) depending on the initial temperature, the pressure level, the temperature jump and cooling (heating) scenario. Moreover, the kinetics of water vapour adsorption and desorption has been measured for the same loose grains under two typical boundary conditions of adsorption heat pumps.

2. Experimental apparatus, procedure, and materials

2.1. Apparatus

The sorption kinetics' setup consists, as depicted in Fig. 2, mainly of two compartments. The first is the measuring cell, in which a sorbent sample is placed. The temperature of the surface holding the sample can be adjusted and controlled using an oil

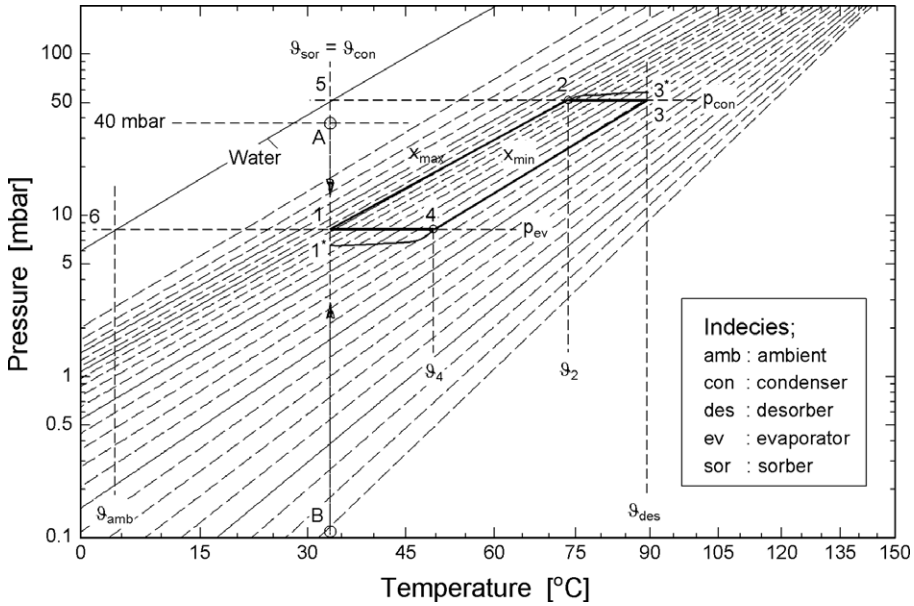

Fig. 1. Schematic of the old and new measuring methodologies on a vapor pressure diagram for system "SWS-1L-water".

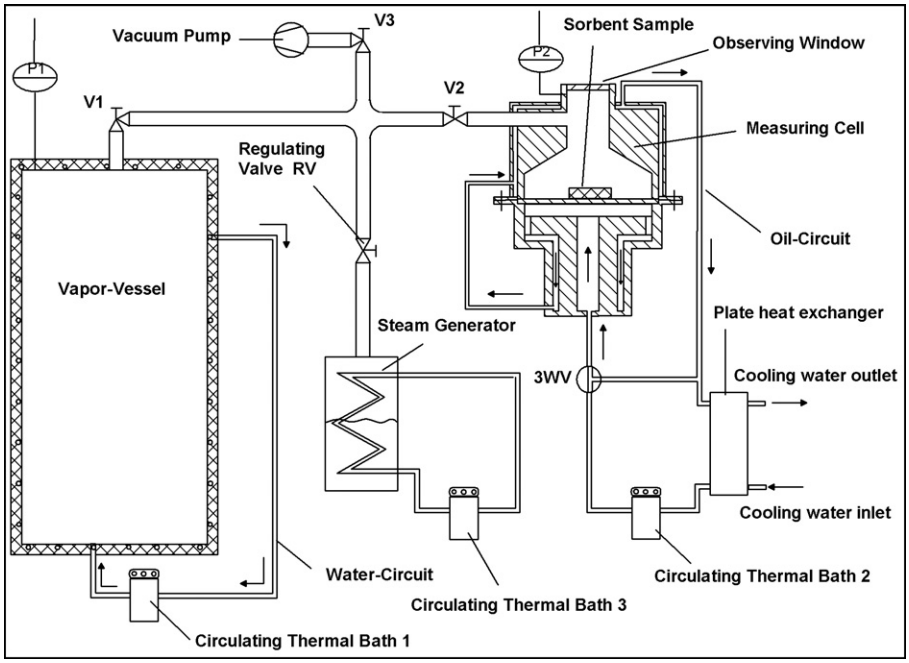

Fig. 2. Schematic diagram of the modified kinetic setup.

circuit coupled to the circulating heating thermal bath 2. The rate of oil heating and cooling can be adjusted by moderating the cooling water flux, which circulates through the plate heat exchanger, so that different cooling (heating) scenarios can be realized. The second compartment is a constant volume vapour vessel. The temperature of this vessel is controlled using a water circuit coupled to the circulating thermal bath 1. This bath 1 is also used to control the temperature of the outer surface of the connecting pipes of the setup (not shown in Fig. 2) to prevent the undesired local vapour condensation. A heating/cooling bath 3 is added to adjust the temperature, and consequently, the pressure of water vapour in the steam generator, in order to obtain the equilibrium state at the beginning of the adsorption and desorption processes, respectively. A three way valve (3WV) is introduced in the oil loop to bypass the measuring cell and first heat or cool the oil content of the thermal bath 2 to the desired final temperature for the desorption or adsorption processes, respectively. By rotating the 3WV to the position, which enables the heated/cooled oil to flow into the measuring cell, either a desorption or an adsorption process could be started.

2.2. Experimental procedure

The sorbent sample was heated to 100 °C and evacuated for one hour using a vacuum pump (valves V1–V3 are open, valve RV is closed). Valve V3 is then closed and the measuring cell is cooled down to the starting temperature of the isobaric adsorption stage ϑ_4 (point 4, Fig. 1). The vapour vessel and measuring cell are charged with water vapour, from the steam generator, up to the required starting pressure for the adsorption process (P_{ev}). The temperature of the connecting piping and valves was maintained for isobaric adsorption at 35 °C, while for isobaric desorption at 50 or 60 °C. When the sample had been equilibrated with water vapour at ϑ_4 and p_{ev}, the measuring cell is cooled down to ϑ_1 with two different cooling scenarios: fast (for the most of experiments) and slow (for a few selected experiments) cooling.

The adsorption process driven by the sample cooling started, that results in reducing the vapour pressure with time (process 4–1* schematically in Fig. 1). This decrease did not exceed 2–3 mbar, which is quite typical for adsorption heat pumps, as the evaporator could not be designed to keep the pressure perfectly constant, most specifically, at the beginning of the adsorption process. Accordingly, the adsorption process can be considered as a quasi-isobaric one as it proceeded close to isobaric line 4–1 (Fig. 1). The pressure variation, being measured with two pressure transducers P1 and P2 is used to determine the amount of the adsorbed water vapour on the sorbent sample (see the next section). The accuracy of the pressure measuring system, being applied, amounts to ±0.05 mbar. The temperature controllers of the circulating thermal bathes have an accuracy of ±0.1 K. Similar procedure was used for studying the dynamics of water desorption which was quasi-isobaric and closely followed line 2–3* (Fig. 1). Table 1 presents the boundary conditions of the performed tests on the loose SWS grains.

The sorption process approaches the equilibrium state related to the final water vapour pressure $p_f < p_{ev}$ and the final sample temperature ϑ_1. The sample mass was minimized in a way to ensure that the final pressure p_f differs from p_{ev} by not more than ±5% along line 2–3* and ±15% along line 4–1*. In our apparatus the weight was fixed at 100 mg. This allowed us to consider the adsorption process as a quasi-isobaric one. The data required for evaluating the change of water uptake with time were recorded every second.

2.3. The tested sorbent

The tested composite SWS-1L was synthesized by impregnating $CaCl_2$ into mesoporous silica gel according to the common procedure described in [7]. The salt content amounts to 33.7 wt.% (dry base). The average pore diameter and specific area of the sorbent amount to 15 nm and 230 m^2/g, respectively. The grain size was between 1.4 and 1.6 mm.

3. Analysis of the experimental test-rig

A water vapour mass balance on the measuring cell of the sorption kinetics setup yields

Table 1
Experimental conditions (temperature of the evaporator ϑ_{ev}, initial ϑ_o and final ϑ_f temperatures of the metal plate, the change in uptake Δx and ΔN), characteristic times τ and maximum condenser/evaporation power W_{max} for the grain size 1.4–1.6 mm

Run	ϑ con/ϑev, °C	$\vartheta_o \Rightarrow \vartheta_f$, °C	τ, s	$\Delta x = x_f - x_o$, g/g	$N_f - N_o$, mole/mole	W_{max}, kW/kg
1	30	60 ⇒ 90	160	−0.24 = 0.11–0.35	2.0 –6.4	3.7
2	30	90 ⇒ 60	260	0.23 = 0.34–0.11	6.3– 2.0	2.2
3	30	60 ⇒ 70	200	−0.09 = 0.25–0.34	4.6–6.3	1.15
4	30	70 ⇒ 80	160	−0.12 = 0.13–0.25	2.4 –4.6	1.9
5	30	80 ⇒ 90	190	−0.02 = 0.11–0.13	2.0 –2.4	0.27
6	30	90 ⇒ 80	250	0.02 = 0.13-0.11	2.4–2.0	0.23
7	30	80 ⇒ 70	265	0.12 = 0.25–0.13	4.6–2.4	1.1
8	30	70 ⇒ 60	265	0.09 = 0.34–0.25	6.3–4.6	1.1
9	10	60 ⇒ 35	550	0.17 = 0.28–0.11	5.1–2.0	0.8
10	10	35 ⇒ 60	290	−0.17 = 0.11–0.28	2.0–5.1	1.45
11	10	35 ⇒ 45	235	−0.09 = 0.22–0.31	4.1–5.6	0.9
12	10	45 ⇒ 55	600	−0.10 = 0.12–0.22	4.1– 2.2	0.4
13	10	55 ⇒ 45	1340	0.11 = 0.23-0.12	2.2 - 4.1	0.2
14	10	45 ⇒ 35	355	0.08 = 0.30-0.22	5.5–4.1	0.55
15	10	65 ⇒ 35*	–	0.19 = 0.30-0.11	5.5–2.0	0.95
16	10	35 ⇒ 65**	–	−0.19 = 0.11-0.30	2.0 - 5.5	1.4
17	0	55 ⇒ 35	1550	0.12 = 0.23-0.11	4.2– 2.0	0.2

** Low heating rate.
* Low cooling rate.

$$\frac{dm_{WV,MC}}{dt} = |\dot{m}_{WV,VV}| - \dot{m}_{WV,s}. \quad (1)$$

Assuming an ideal gas behaviour for the water vapour during the whole sorption process, both the rate of water vapour flow from the vapour vessel to the measuring cell and the time rate of variation of the mass of the vapour phase in the measuring cell can be obtained according to the following Eqs. (2) and (3)

$$|\dot{m}_{WV,VV}| = \left|\frac{\Delta m_{WV,VV}}{\Delta t}\right| = \frac{m_{WV,VV}(t) - m_{WV,VV}(t+\Delta t)}{\Delta t} = \frac{(p_1(t) - p_1(t+\Delta t)) \cdot V_{VV}}{R_{WV} \cdot T_{VV} \cdot \Delta t}, \quad (2)$$

$$\frac{dm_{WV,MC}}{dt} = \frac{(m_{WV,MC}(t+\Delta t) - m_{WV,MC}(t)}{\Delta t} = \frac{(p_2(t+\Delta t) - p_2(t)) \cdot V_{MC}}{R_{WV} \cdot T_{MC} \cdot \Delta t}. \quad (3)$$

Combination of Eqs. (1)–(3) gives the mass rate of the water sorption according to Eq. (4):

$$\dot{m}_{WV,s} = \frac{\Delta m_{WV,s}}{\Delta t} = \frac{(p_1(t) - p_1(t+\Delta t)) \cdot V_{VV}}{R_{WV} \cdot T_{VV} \cdot \Delta t} - \frac{(p_2(t+\Delta t) - p_2(t)) \cdot V_{MC}}{R_{WV} \cdot T_{MC} \cdot \Delta t} \quad (4)$$

Rewriting Eq. (4) in Eq. (5) gives an expression for the amount of the sorbed water vapour on the sorbent sample

$$\Delta m_{WV,s} = \frac{|\Delta p_1| \cdot V_{VV}}{R_{WV} \cdot T_{VV}} - \frac{\Delta p_2 \cdot V_{MC}}{R_{WV} \cdot T_{MC}}. \quad (5)$$

Knowing the mass of the dry sorbent sample $m_{S,dry}$ as well as the starting water loading x_o, the time variation of the water loading can be calculated

$$x = x_o + \sum_{t=0}^{t} \frac{\Delta m_{WV,s}}{m_{S,dry}} \quad (6)$$

In order to compare the results of the sorption and desorption kinetics under different operating conditions, it is reasonable to represent the time variation of the water loading in a dimensionless form. This may occur by defining the dimensionless differential water loading χ as the ratio between the instantaneous differential water loading to the maximum differential water loading achievable at each operating condition of each sorption and desorption process on the sorbent sample

$$\chi_t = \frac{x_t - x_o}{x_f - x_o} \quad (7)$$

A detailed error analysis for the accumulated error in estimating the absolute water loading showed a maximum error of ±0.008 g/g that leads to the accuracy of calculating the differential water loading was typically equal to ±0.015. This accuracy is quite reasonable although for the future work the accuracy of pressure measurment should be improved to 0.01–0.02 mbar instead of 0.05 mbar in order to damp the fluctuation and allow one to measure even smaller differential water loadings.

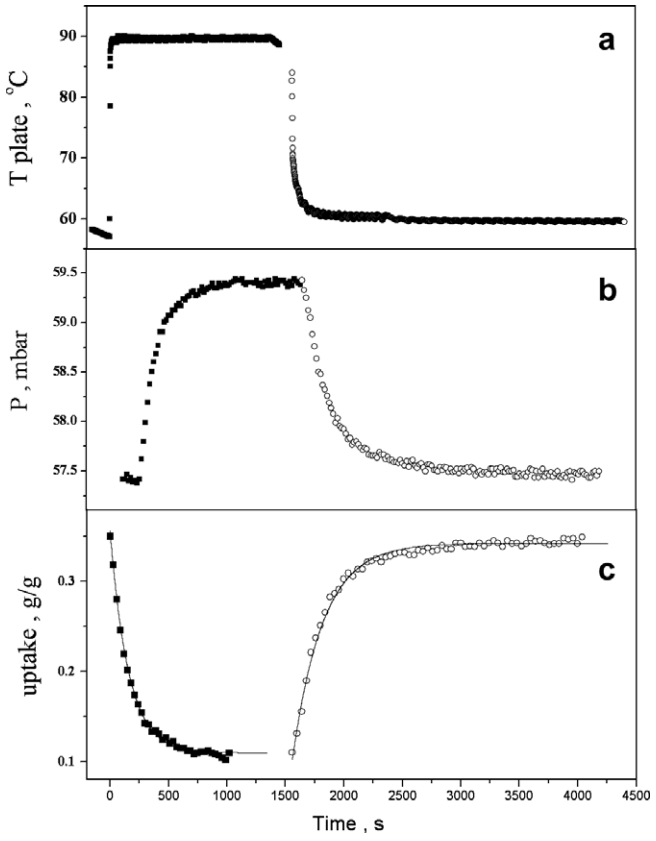

Fig. 3. The temperature evolution of metal plate (a), the pressure over the sample (b) and the water uptake (c) for cooling (open circle) and heating (solid square) runs. The solid line is exponential approximation $m_t = m_o + (m_f - m_o)(1 - \exp(-t/\tau_o))$. Runs 1 and 2.

4. Results and discussion

Typical evolution of the surface temperature of the metal plate and the vapour pressure over the sample is presented on Fig. 3, a-c for a fast heating run (run 1 in Table 1) followed by a fast cooling run (run 2 in the same table). The heating run simulates process 2–3* on Fig. 1, while the cooling run has been performed to check the accuracy of the measuring system upon reversing the process direction. Moreover, such a reversed process becomes of interest for a heat transformation process, in which the adsorption process takes place at the higher cycle pressure in order to obtain a higher temperature than that applied for the desorption process, which then takes place at the lower cycle pressure. It can be easily noticed that after initiating the fast cooling (heating) process, the temperature of the holding surface reaches the final temperature ϑ_f, which equals the temperature of the heat carrier (oil) within 1 min. Setting of the equilibrium pressure p_f required, however, much longer time (5–30 min). This can be attributed to the relatively slow kinetics of water desorption/sorption determined by the coupled heat and mass transfer to and inside the sorbent grains. The time course of variation of P(t) (Fig. 3b) allows the calculation of the water uptake as a function of time (Fig. 3c). For most of the fast runs the shape of kinetic curves is near-exponential (Fig. 3c), and the water uptake can be well described as

$$m_t = m_o + (m_f - m_0) \cdot (1 - \exp(-t/\tau)) \quad (8)$$

or

$$\frac{m_t - m_0}{m_f - m_0} = (1 - \exp(-t/\tau)) \quad (9)$$

Equations similar to Eqs. (8) and (9) can be directly derived from the Linear Driving Force Model [8] which considers the rate of adsorption as

$$\frac{dm}{dt} = -k \cdot (m_t - m_f), \quad (10)$$

where the rate constant ($k = 1/\tau$) does not change during the process (k = const). This model commonly describes the kinetics of adsorption process for which the driving force is the difference between the average current and the equilibrium concentrations of an adsorbate [8]. The constant value of k indirectly assumes that the process is isothermal.

The exponential kinetic law (9) differs from the equation $(m_t - m_0)/(m_f - m_0) = A \cdot \sqrt{t}$ found in Ref. [9] for the initial stage of the isothermal and isobaric adsorption (desorption) of water on loose grains of SWS-1L. It was found in [9] that the sorption kinetics was controlled by the Knudsen diffusion of water vapour in the mesopores of SWS grains, while the heat transfer was very fast and did not affect the kinetics.

In this study a near-exponential uptake curves were found under conditions which were almost isobaric but strictly non-isothermal. We may suppose that such behaviour is likely a result of complex action of coupled processes of heat and mass transfer that takes place under non-steady state conditions of our experiments. Indeed, at the beginning of the heating process ($t = 0$, $T_{gr} = T_o$, $T_{pl} = T_o + \Delta T$) the driving force for the heat transfer, that is the temperature difference ΔT between the plate and the grains, is maximum. At this moment the driving force for the mass transfer equals zero. This stimulates the fast grain heating ($T > T_o$) which results in the desorption of water and the increase of the pressure inside the grain. The pressure gradient is the driving force for water diffusion from the grain, which alters the uptake and water distribution inside the grain. The heat consumed to remove water alters the grain temperature and so on. For better understanding of this complicated process a detailed mathematical modelling of the heat and mass transfer in this system has been performed [10].

The characteristic times τ of sorption process for the SWS grains of 1.4–1.6 mm size are displayed in Table 1. Along the high pressure line 2–3 (ϑ_{con} = 30 °C) the typical value of τ is between 160 and 260 s, that is smaller than along the low pressure line 1–4 (ϑ_{ev} = 10 °C) τ = 230–1350 s. Even slower process was observed at ϑ_{evm} = 0 °C (Table 1) with τ = 1560 s.

For several runs experimental kinetic curves can not be adequately described by Eq. (8), for instance, runs 5, 6, 10 and 12 (Fig. 4). We do present in Table 1 the characteristic times for the best exponential fit of these kinetic curves for convenient comparison with other runs. As for all these runs either the initial or final uptake corresponds to a solid crystalline hydrate $CaCl_2 \cdot 2H_2O$, the deviation from exponential behaviour can be interpreted by peculiarities of a gas-solid reaction $CaCl_2 \cdot 2H_2O + 2H_2O \Leftrightarrow CaCl_2 \cdot 4H_2O$.

The factors, that can influence the sorption kinetics and, hence, the its characteristic time, are the rate of cooling of metal plate, the heat transfer between the plate and adsorbent grains, the heat and mass transfer inside the grains as well as the rate of chemical reaction between the salt and water.

4.1. Influence of the process temperature

Although only desorption runs from 60 to 90 °C at P = 56–58 mbar and adsorption runs from 60 to 35 °C at P = 10–12 mbar are of practical interest, we also measured the kinetics of reverse runs (means, adsorption runs from 90 to 60 °C at P = 56–58 mbar and desorption runs from 35 to 60 °C at P = 10–12 mbar) in order to elucidate the effect of process temperature on sorption kinetics. Indeed, it is well known that the rate of sorption is commonly temperature dependent [11]. Considering direct and reverse temperature jumps (for instance, fast heating from 60 to 90 °C (run 1) and fast cooling from 90 to 60 °C (run 2)), it can be seen that the characteristic time τ is always smaller for desorption stage (Table 1). This can be attributed to higher average temperature of the metal plate during desorption runs. Indeed, it reaches the temperature of the heat carrier in about 1 min. (Fig. 3) that could result also in higher average grain temperature. This is solely an assumption as the temperature of the isolated SWS grains has not been directly measured during these experiments.

If one, for simplicity, neglects the short transient stage and assumes that the heating (cooling) process was very fast so that the sorption process is quasi-isothermal and proceeded at the final plate temperature (means, 90 °C for desorption and 60 °C for adsorption at P = 56–58 mbar), it is easy to estimate the apparent activation energy of the process. For instance, for adsorption run 2, which is supposed to proceed mostly at T_1 = 60 °C, the character-

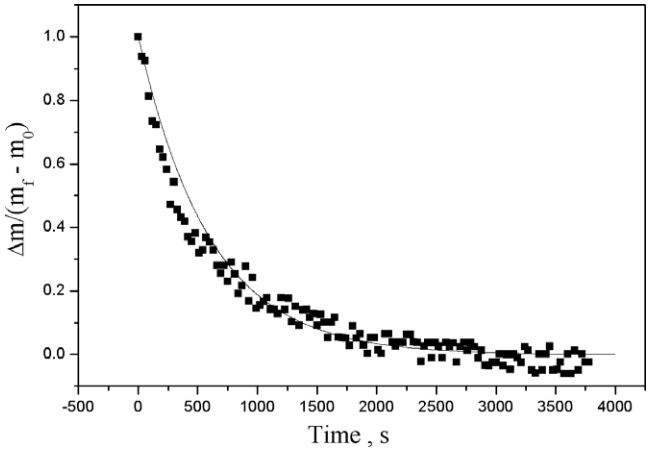

Fig. 4. Exponential fit of the experimental kinetic curve corresponding to run 12.

istic time is $\tau(T_1) = 260$ s, while for desorption run 1 with the same temperature jump, which is supposed to proceed mostly at $T_2 = 90$ °C, $\tau(T_2) = 160$ s. If we assume that the temperature dependence of τ is the Arrhenius one [11] $\tau(T) = \tau_o \exp(-E_{act}/RT)$, the apparent activation energy of the process can be briefly estimated as 17 ± 2 kJ/mol. So calculated values of E_{act} are displayed for selected temperature jumps in Table 2. The tendency is that E_{act} is larger at low average uptakes and smaller at high average uptakes, that correlates well with the apparent activation energy of the rate constant of water diffusion in the SWS-1L pores measured in [9]: $E_a = 60 \pm 6$ kJ/mol at $N \approx 2$–3 and 28 ± 4 kJ/mol at $N > 4$.

4.2. Influence of the cooling (heating) scenario

For the fast heating the metal plate became isothermal in 50–100 s, while for the slow one, it took 300 s and 500 s for the heating and cooling, respectively (Fig. 5). As a result, the uptake change was much slower than for the fast temperature change. Especially large difference was observed at the initial part of uptake curve, which was essentially non-exponential (Fig. 5c). To analyse such kinetics it is worthy to introduce the characteristic times $\tau_{0.5}$ and $\tau_{0.9}$, which correspond to 50% and 90% of reaching the equilibrium loading (Table 3). It could be easily noticed that the $\tau_{0.5}$-time is much longer for the slow temperature change, while the $\tau_{0.9}$-times are almost equal, especially for cooling mode. Thus, a cooling scenario affects the beginning of uptake curve more than its tail.

4.3. Evaluation of the maximum specific power

Eq. (11) gives the instantaneous specific power $W(t)$ which is released in the condenser or consumed in the evaporator due to water desorption (adsorption) in an adsorption heat pump.

$$W = h_{fg}(dm/dt)/m_{ads} = [h_{fg}(m_\infty - m_o)/(\tau m_{ads})]\exp(-t/\tau) = W_{max}\exp(-t/\tau) \quad (11)$$

Herein, h_{fg} is the latent heat of evaporation of liquid water taken as 2478 J/g, m_{ads} is the mass of dry adsorbent [g], $W_{max} = \Delta H\,(m_\infty - m_o)/(\tau\, m_{ads})$ is the maximum specific power which is released at $t \Rightarrow 0$. Even for large SWS grains (1.4–1.6 mm) at heating stage (2–3) it can reach 3.7 kW/kg_{ads} at the vapour pressure 55–60 mbar. For water adsorption at low vapour pressure (10–15 mbar) the maximum power is lower (0.75–1.9 kW/kg_{ads}).

The average power within the time interval $[0, t]$ is

$$W_t = \frac{1}{t}\int_0^t W_t.dt = W_{max}\cdot\frac{\tau}{t}\cdot[1-\exp(-t/\tau)]. \quad (12)$$

At $t \Rightarrow 0$ $W_t = W_{max}$, while at $t = \tau_{0.9} = 2.3\tau$ $W_t = 0.391 W_{max}$. It means that waiting for 90% of the water sorption equilibrium, one can still obtain quite high average specific power which is only 2.6 times lower than the maximum values displayed in Table 1. As the shape of the uptake curves is not strictly exponential but only almost exponential, this figures should be considered as an estimation especially as concerned the time for reaching 90% of equilibrium.

Thus, our experiments give the experimental evidence for the possibility to build quite compact adsorption cooling/heating devices which utilize loose grains of SWS-1L. One can expect higher specific power in the case of a compact layer prepared with a binder and consolidated with metal surface of heat exchanger.

Table 2
Apparent activation energy estimated from direct and reverse temperature jumps

Runs	ϑ con/ ϑev, °C	$\vartheta_o \Leftrightarrow \vartheta_f$, °C	$N_o \Leftrightarrow N_f$ mole/mole	E_a, kJ/mol
1, 2	35	60 ⇔ 90	2.0 ⇔ 6.3	17
3, 8	35	60 ⇔ 70	4.6 ⇔ 6.3	35
4, 7	35	70 ⇔ 80	2.4 ⇔ 4.6	39
9, 10	10	35 ⇔ 60	2.0 ⇔ 5.1	22
11, 14	10	35 ⇔ 45	4.1 ⇔ 5.5	33
12, 13	10	45 ⇔ 55	2.2 ⇔ 4.1	70

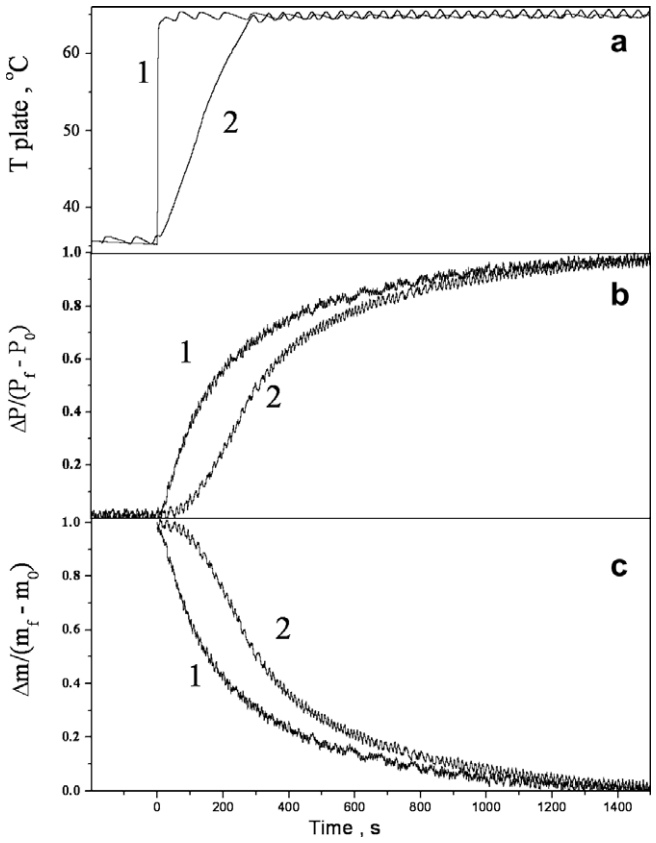

Fig. 5. The temperature evolution of metal plate (a), the pressure over the sample (b) and the water uptake (c) for different heating scenario: 1 fast and 2 low. Runs 10 and 16.

Table 3
Characteristic times $\tau_{0.5}$ and $\tau_{0.9}$ of the water adsorption (desorption) for the fast and slow cooling (heating)

Run	Heating/cooling mode	$\vartheta_o \Rightarrow \vartheta_f$, °C	$\tau_{0.5}$, s	$\tau_{0.9}$, s
10	Fast heating	35 ⇒ 6o	160	730
16	Slow heating	35 ⇒ 65	310	910
9	Fast cooling	60 ⇒ 35	420	1300
15	Slow cooling	65 ⇒ 35	680	1370

$\Delta x = 0.28$–$0.11 = 0.17$ g/g, $\Delta N = 5.1 - 2.0 = 3.1$ mole/mole.

5. Conclusions

In this paper we proposed and tested a new methodology of studying the kinetics of water vapour sorption/desorption under operating conditions which are very close to those realised during isobaric stages of real adsorption heat pumps. The measurements have been carried out on pellets of composite sorbent SWS-1L ($CaCl_2$ in silica KSK) placed on a metal plate. Temperature of the plate was changed as it takes place in real sorption heat pumps, while the vapour pressure over the sorbent was maintained almost constant. Near-exponential behaviour of water uptake on time was found for most of the experimental runs. Characteristic time τ of isobaric adsorption (desorption) was measured for one layer of loose grains having a size between 1.4 and 1.6 mm for different heating/cooling scenarios and boundary conditions of adsorption heat pump. Maximum specific power estimated from the τ-values

can exceed 1.0 kW/kg of dry adsorbent, that gives proof to the idea of compact adsorption units for energy transformation with loose SWS grains.

Acknowledgement

This work was supported by INTAS (grant 03-51-6260), RFBR (grants 05-02-16953, 07-08-13620 and 08-08-00808) and DAAD (Guest Research Fellowship of 2003) for partial financial support.

References

[1] R. Lang, M. Roth, M. Stricker, Development of a modular zeolite-water heat pump, in: Proceeding of International Sorption Heat Pump Conference ISHPC 99, Munich, Germany, 1999, pp. 611–618.
[2] M. Stricker, Entwicklung einer mehrmodularen Zeolith-Wasser-Adsorptionswärme-pumpe, PhD thesis, RWTH Aachen University, VDI Verlag, Germany, 2003.
[3] B. Dawoud, Yu.I. Aristov, Experimental study on the kinetics of water vapour sorption on selective water sorbents, silica-gels and alumina under typical operating conditions of sorption heat pumps, Int. J. Heat Mass Transfer 46 (2) (2003) 273–281.
[4] B. Dawoud, J. Pfeiffer, Yu.I. Aristov, Kinetics of water sorption on sorbent "$CaCl_2$ in silica" under typical conditions of an adsorption heat pump; Influence of the grain size, in: Proceeding of V Minsk International Seminar Heat Pipes, Heat Pumps, Refrigerators, Minsk, Belarus, 2003, pp. 306–314.
[5] L. Schnabel, H.-M. Henning, Experimental and simulation study on the kinetics of water vapor adsorption on different kinds of adsorptive material matrices, in: Proceeding of the International Conference on Sorption Heat Pumps, ISHPC05, June 22–24, Denver, CO, USA, Paper No. 39, 2005, pp. 1–8.
[6] L. Schnabel, G. Munz, H.-M. Henning, Experimental study on the kinetics of water vapor adsorption, OTTI in: Proceedings of the International Conference on Solar Air Conditioning, October 6th to 7th, Kloster Banz, Bad Staffelstein, Germany, 2005.
[7] Yu.I. Aristov, M.M. Tokarev, G. Cacciola, G. Restuccia, Selective water sorbents for multiple applications: 1. $CaCl_2$ confined in mesopores of the silica gel: sorption properties, React. Kinet. Catal. Lett. 59 (2) (1996) 325–334.
[8] E. Glueckauf, Part 10. Formulae for diffusion into spheres and their application to chromatography, Trans. Faraday Soc. 51 (11) (1955) 1540–1551.
[9] Yu.I. Aristov, I.S. Glaznev, A. Freni, G. Restuccia, Kinetics of water sorption on SWS-1L (calcium chloride confined to mesoporous silica gel): influence of grain size and temperature, Chem. Eng. Sci. 61 (5) (2006) 1453–1458.
[10] B.N. Okunev, L.I. Heifets, Yu.I. Aristov, A new methodology of studying the dynamics of water sorption/ desorption under real operating conditions of adsorption heat pumps: Modelling of coupled heat and mass transfer, Int. J. Heat Mass Transfer 51 (2008) 246–252.
[11] J. Kaerger, D.M. Ruthven, Diffusion in Zeolites and Other Microporous Solids, second ed., John Wiley & sons, New York, 1994.